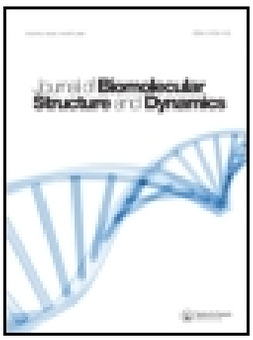

Taylor & Francis
Taylor & Francis Group

Journal of Biomolecular Structure and Dynamics

ISSN: (Print) (Online) Journal homepage: https://www.tandfonline.com/loi/tbsd20

Oxidative polymerization of hydroxytyrosol catalyzed by laccase, tyrosinase or horseradish peroxidase: influencing factors and molecular simulations

Pujun Xie , Linlin Fan , Lixin Huang & Caihong Zhang

To cite this article: Pujun Xie , Linlin Fan , Lixin Huang & Caihong Zhang (2020): Oxidative polymerization of hydroxytyrosol catalyzed by laccase, tyrosinase or horseradish peroxidase: influencing factors and molecular simulations, Journal of Biomolecular Structure and Dynamics, DOI: 10.1080/07391102.2020.1801512

To link to this article: https://doi.org/10.1080/07391102.2020.1801512

Published online: 11 Aug 2020.

JOURNAL OF BIOMOLECULAR STRUCTURE AND DYNAMICS
https://doi.org/10.1080/07391102.2020.1801512

Taylor & Francis
Taylor & Francis Group

Oxidative polymerization of hydroxytyrosol catalyzed by laccase, tyrosinase or horseradish peroxidase: influencing factors and molecular simulations

Pujun Xie[a,b], Linlin Fan[c], Lixin Huang[b] and Caihong Zhang[b]

[a]Institute of New Technology of Forestry, Chinese Academy of Forestry, Beijing, China; [b]Institute of Chemical Industry of Forest Products, Chinese Academy of Forestry; National Engineering Laboratory for Biomass Chemical Utilization; Key and Open Laboratory on Forest Chemical Engineering, National Forestry and Grassland Administration, Key Laboratory of Biomass Energy and Material, Nanjing, China; [c]Institute of Agro-product Processing, JAAS, Nanjing, China

Communicated by Ramaswamy H. Sarma

ABSTRACT

Hydroxytyrosol oligomer from bioenzymatic catalysis indicates a pleiotropic wellness improving (e.g. antioxidation, anti-inflammatory and anti-carcinogenesis) than its monomer. However, the processing parameters and the insightful mechanism of hydroxytyrosol polymerization are still lacking. To explore in detail the process of hydroxytyrosol polymerization, the effects of different reaction factors (solvent type, pH value of reaction solution, reaction temperature and time) on the polymerization yield were investigated, and molecular docking was executed to reveal the relevant structural variations of these enzymes. The results showed hydroxytyrosol polymerization implemented by laccase performed the best at 50 °C for 20 min in the aqueous buffer solution of pH 5.0. The docking results demonstrated PRO4, TYR7, ASP8, PRO12, LEU121 and VAL14 in site 9 of laccase interacted with hydroxytyrosol in hydrogen bonding, pi-sigma, pi-alkyl and van der Waals' force. Moreover, the molecular dynamic results implied their interaction-energy variation reaching balance within 175 *ps*, which confirmed the enzymes' structural changes. Meanwhile, structural analysis in torsion and bond lengths showed that the C–O of phenolic bonds from hydroxytyrosol evidently rotated and its length of the relevant O–H became longer when binding to laccase compared with free hydroxytyrosol. All the findings are helpful to strengthen the understanding for the enzymatic polymerization of catechol-based structures and the resulting *o*-dihydroxy-grafting oligomers could be potentially used in the field of functional foods, cosmetics and pharmaceuticals, even or an innovative bioenzyme design such as biosensor for measuring phenols in industrial effluent or preparing the singular oligomer oriented is worth being explored in future.

ARTICLE HISTORY
Received 23 April 2020
Accepted 25 June 2020

KEYWORDS
Laccase; enzymatic polymerization; hydroxytyrosol oligomers; process parameters; molecular dockings and dynamics

1. Introduction

Both laccase and tyrosinase related to Cu-based enzyme active region, and horseradish peroxidase related to Fe-based enzyme active region, are widely distributed in plants and fungi and exploited in numerous studies owing to their high efficiency and accessible obtaining for treating phenolic compounds into polymerization (Awasthi et al., 2015; Bilal et al., 2019; Dec & Bollag, 1990; Durán & Esposito, 2000; Litescu et al., 2010; Roberts et al., 2016; Solná & Skládal, 2005; Stadlmair et al., 2018). Their enzyme-catalytic mechanisms are involved in turning two molecules of oxygen into water in the wake of a four-electron reduction that a radical species is produced by the oxidized substrate with one electron, and then generates a polymer by a chain reaction among radicals (Shleev et al., 2006; Shoda et al., 2016). Among them, fungal laccases such as *Coriolus versicolor* commonly show a higher reactive property than plant laccases although they have a similar structure, reckless of their originals (Pinheiro et al., 2020; Solomon et al., 2008). Tyrosinases are easily prepared from mushroom and are capable of making monophenols *o*-hydroxylated and *o*-diphenols become *o*-quinones subsequently (Liu et al., 2020). Horseradish peroxidase containing protoheme group, generates the polymerization for abundant phenolics in favor of hydrogen peroxide (Shalit et al., 2019).

One of the most challenging tasks in the field of olive industry around the world comes from how to make effective treatments of olive mill wastewater and olive pomace in addition to extracting olive oil. Environment polluting (e.g. soil damage) and resource wasting were produced if the olive byproducts were discarded directly. Actually, olive mill wastewater and olive pomace consist of abundant phenolic compounds (secoiridoids such as hydroxytyrosol, oleuropein, dimethyl-oleuropein, verbascoside and comselogoside; flavonoids such as apigenin, cyanidin flavone, anthocyanin and quercetin; phenolic acids such as caffeic, ferulic, gallic, chlorogenic and protocatechuic acid) with *o*-dihydroxyl phenolics-based in an overwhelming majority (Araújo et al., 2015; Paulo & Santos, 2020). However, hydroxytyrosol, dominates the olive mill wastewater and olive pomace treatment

CONTACT Lixin Huang l_x_huang@163.com Institute of Chemical Industry of Forest Products, Chinese Academy of Forestry, No. 16 Suojin wucun, Xuanwu District, Nanjing, Jiangsu Province 210042, China

among phenolic compounds reaching an approximate 70% (Duran & Esposito, 2000). Using bioenzymes such as laccase, tyrosinase and horseradish peroxidase enable to not only highly improve the (bio)chemical-oxygen-demand level of the olive mill wastewater but also enrich phenolic oligomers as invaluable fine chemicals for industrial applications (Sarkar et al., 2020; Torres et al., 2003; Wang et al., 2020). For instance, laccase enables to make a self-polymerization of hydroxytyrosol produce its dimer, trimer, tetramer, etc. (Zwane et al., 2012), and these hydroxytyrosol oligomers have a better anti-oxidation and stronger protection against UVA radiation action than hydroxytyrosol (Cardinali et al., 2010; Sánchez-Ferrer et al., 1995). The oligomers (degree of polymerization less than 10) have much more superior functions including antioxidation, anti-diabetes, anti-inflammatory, anti-microbials, anti-carcinogens and neuroprotection than the monomer (hydroxytyrosol) itself (Oliver et al., 2016). A preliminary enzyme selection has been examined to allow for employing molecular oxygen in the oxidative polymerization, with a high conversion intensity as well (Ikehata & Nicell, 2000). As above mentioned, these enzymatic-catalysis processes could be described as a scheme in Figure S1. In fact, the polymerized products were also potently dependent on the reaction parameters such as pH value, the reaction temperature and time in the reaction system (Edwards et al., 1999). Previous reports indicated that polyphenols like kaempferol and quercetin can be polymerized by laccase and tyrosinase producing the oligomers with a bigger size and stronger scavenging radicals efficacy on reactive oxygen species and inhibition of lipoperoxidation (Desentis-Mendoza et al., 2006); catechin dimers were yielded by horseradish peroxidase and laccase with 2 ~ 8-fold greater than α-tocopherol and catechin in anti-lipid peroxidation (Hosny & Rosazza, 2002). Free radical induced polymerization of caffeic acid with a trimmer-dominating catalyzed by horseradish peroxidase were achieved (Xu et al., 2005). Thereby, phenolic compounds containing *o*-dihydroxyl can be catalyzed by laccase, tyrosinase and horseradish peroxidase as preliminary resulting products of dimer or trimmer. Additionally, the enzyme-based synthesis indicates some merits: (1) high energetic efficiency in mild reaction conditions (temperature, pressure and pH); (2) superior enantio-, regio- and chemoselectivities for fine chemical applications; (3) natural catalyst with biosafety and 'green' attributes for ecological demand (Kobayashi et al., 2001). Recently, with the rapid advancement of quantum chemistry, theoretical investigations with computing chemistry application in enzyme catalysis is greatly prevalent. Taking into account that quantum chemistry and molecular mechanics for revealing the mechanism of enzymatic catalysis is favorable to acquire the deep observations in the reaction process and a relevantly reasonable explanation. Because the substantial studies on the metal ion (Cu or Fe) in the reaction process of polyphenol oxidases and peroxidase (Marszałek et al., 2017; Zhu et al., 2020) have been carried out, the findings from the other enzymatic structural variations as well as the binding position acting as a catalyzing center during the catalysis are of great importance and also still lacking in the present. Beyond that, to the best of our knowledge, few studies concerning a comprehensive study regarding the reaction process of hydroxytyrosol catalyzed by laccase, tyrosinase or horseradish peroxidase have been found so far. Moreover, the reaction mechanism between hydroxytyrosol and the three enzymes was explored.

Taken together, in combination to our preliminary results that indicated hydroxytyrosol polymerization can occur with the aid of laccase, tyrosinase or horseradish peroxidase, the polymerized products were mostly concentrated in the dimer and trimer of hydroxytyrosol under a weak-acidity aqueous solution system (pH 5.0). Also, the identified polymers presented a C–C bond and a degree of polymerization less than six by FT-IR and ^{1}H-, ^{13}CNMR and HPLC-QTOF-MS (data not shown). However, in view of the environment protection and cyclable economic importance of the enzymatic polymerization of hydroxytyrosol for olive by-products, the processing parameters and the insightful mechanism of hydroxytyrosol polymerization are worthy of being explored. To further reveal the different catalyzation processes of hydroxytyrosol implemented by laccase, tyrosinase or horseradish peroxidase, the effects of different reacting factors such as solvent types (methanol, acetone, water and ethyl acetate) reaction times, reaction temperatures and pH values of the solution were studied in this scenario. Docking and dynamic simulations *in silico* were used to reveal the molecular structure changes of the enzyme in the oxidative polymerization processes.

2. Materials and methods

2.1. Enzymes and chemicals

Hydroxytyrosol, 2, 2′-azino-bis (3-ethylbenzothiazoline-6-sulfonic acid) (ABTS), *L*-tyrosine, pyrogallol and laccase (EC number: 1.10.3.2) produced by *Coriolus versicolor*, tyrosinase (EC number: 1.14.18.1) and horseradish peroxidase (EC number: 1.11.1.7) were purchased from Sigma-Aldrich Inc. (St. Louis, MO, USA). Other agents in this study were purchased from Nanjing Chemical Reagents Inc. (China). Different pH buffers such as pH 4.0 (0.05 M $C_8H_5KO_4$-NaOH), pH 5.0 (0.1 M HAC-NaAC), pH 5.8 (0.05 M KH_2PO_4-K_2HPO_4) and pH 6.8 (0.025 M Phosphate Buffer Solution, PBS) are prepared accordingly. Besides, the data including molecular weight and enzyme activity of laccase (60 kD, 121.5 U/mL), tyrosinase (126.5 kD, 28.75 U/mL) and horseradish peroxidase (35 kD, 25.1 U/mL) were obtained (Table S1), calibrated at 25 °C by the substrates of ABTS, *L*-dopa and pyrogallic acid at the conditions of pH 5.0, 5.8 and 5.0, measurement wavelengths of 420, 475 and 420 nm, respectively.

2.2. Enzymatic oxidative-polymerization of hydroxytyrosol with laccase, tyrosinase or horseradish peroxidase

The oxidative polymerization of hydroxytyrosol assay mixture contains 1.0 mL of 5.0 mM hydroxytyrosol solution, 1.0 mL of 8.0 μM solutions for each enzyme (laccase, tyrosinase or

horseradish peroxidase) dissolved by a pH-buffered solution, 10 mL of different pH-buffered solutions and 10 mL of distilled water. About 0.5 mL of H_2O_2 (30%, v/v) was added into this reaction system when horseradish peroxidase was applied. Moreover, specific operating conditions for laccase, tyrosinase or horseradish peroxidase were investigated on different solvent systems (methanol, acetone, ethyl acetate and aqueous buffer solution), reaction temperatures (30, 40, 50 and 60 °C) and time (10, 20, 40 and 60 min) and pH values (4.0, 5.0, 5.8 and 6.8). The experiments were magnetically stirred at 180 rpm in an opening Erlenmeyer flask. The resulting samples were taken periodically and analyzed by UV/Vis spectrum (T6, Beijing, China) at a full scanning. Also, the dissolved oxygen content in the pH-buffered water plus opening equipment was sufficient to treat hydroxytyrosol.

2.3. Molecular docking study

The program Accelrys Discovery Studio v4.0 (Biovia, San Diego, USA) was harnessed to the molecular docking between laccase, tyrosinase or horseradish peroxidase and hydroxytyrosol. The structure optimization of hydroxytyrosol for searching one minimizing energy was achieved by MMFF forcefield. Two settings containing 5000 of maximal paces and 0.1 RMS gradients with an algorithm of smart minimizer were implemented. The 3D structures of laccase (PDB ID: 2HZH), mushroom tyrosinase (PDB ID: 2Y9X) and horseradish peroxidase (PDB ID: 2YIJ) retrieved from a protein databank (PDB; www.rcsb.org). After completing these fundamental preparations, the docking technique was implemented by the Libdock module in the program. The explicit steps were described as the five facets: (i) defining laccase, tyrosinase or horseradish peroxidase molecules as a receptor, (ii) identifying the sites (hotspot) from the receptor cavities (searched for 24 sites, 32 sites and 9 sites in all, respectively), (iii) defining spherical radiuses ranging from 3 to14 Å in the selected site dependent upon the cavity size, (iv) beginning to conduct it to discover the greatest pose according to the highest LibDock score among the sites produced automatically and (v) hunting for the receptor–ligand interaction, for example, hydrogen bonds. What is more, all the sizes of the active site in these enzymes were defined as 2.5 Å with the spacing valued at 0.5 Å. Docking results were ascribed to the different scoring functions. The best scoring indicated the most suitable ligand (hydroxytyrosol) conformation for well-matching with the spots district (internal cavity of the relevant enzyme) between them based on the most suitable spatial-geometric matching and the lowest interactive total energy, and that was considered to be the most reasonable binding behavior between hydroxytyrosol and the enzyme.

2.4. Molecular dynamic simulations

One ligand from hydroxytyrosol with the best docking score when docked with laccase, tyrosinase or horseradish peroxidase was chosen for molecular dynamic (MD) simulation investigations. The selected ligand-protein complexes were implemented by MD simulation run for 224 *ps* via the 'Standard Dynamics Cascade' procedure of Discover Studio v.4.0 which incorporated two steps of minimization followed by heating, equilibrium and production run. CHARMm forcefield was largely employed in a complex of protein–ligand and subsequently permeated in water to simulate an aqueous surrounding. Both the models containing water and spherical boundary solvation with symphonic limitations were greatly unambiguous to practice for this reason. The solvation-sphere radius is fixed at 20 Å. Ahead of MD simulation, energy minimization dealing with the solvated complex through the steepest descent, and an ensuing 5000-step gradient algorithm were executed, with other settings in default. Next, an MD simulation of 224 *ps* was run for the treated ligand–protein complex by NPT. Leapfrog verlet algorithm used as a dynamic integrator was carried out when undergoing SHAKE constraints for the simulation. Target temperature at 323 K and reference pressure at 1.0 bar was sustained during the course of the simulation. The trajectory of each ligand–protein complex was recorded every 2.24 *ps* for analysis of RMSD and RMSF by the module 'Analyze Trajectory' in DS.

2.5. Torsion analysis

Based on the best docking site and molecular dynamics results, torsion analyses concerning free hydroxytyrosol and hydroxytyrosol binding with bioenzymes (laccase, tyrosinase and horseradish peroxidase) were implemented. Meanwhile, their bond lengths between the free status and the binding with the bioenzymes of hydroxytyrosol were compared for structural analysis as well.

2.6. Statistics

All the experiments were carried out in triplicate and the data in this text were expressed as means values ± standard deviation, which were calculated by Excel 2016.

3. Results and discussion

3.1. Process optimization in the enzymatic polymerization of hydroxytyrosol

3.1.1. Selection of solvent type

Figure 1(a–c) showed that the UV-Vis absorbance increases under 400 nm were found by using pH 5.0 aqueous buffer solution involving the reactions with laccase, tyrosinase or horseradish peroxidase. Hydroxytyrosol showed one peak at 280 nm due to the π–π^* transitions of the aromatic fragment. In this case of poly(hydroxytyrosol), an extra broader peak was seen at 400 nm which may be attributed to conjugation in the polymer. Intuitively, the resultant solution produced a huge difference from colorless to reddish-brown implying that a successful enzymatic oxidative polymerization was yielded. Because the dissolving hydroxytyrosol in aqueous solution presents colorless at the beginning even when mixed with laccase, tyrosinase or horseradish peroxidase. Also, the products of poly(hydroxytyrosol) presenting

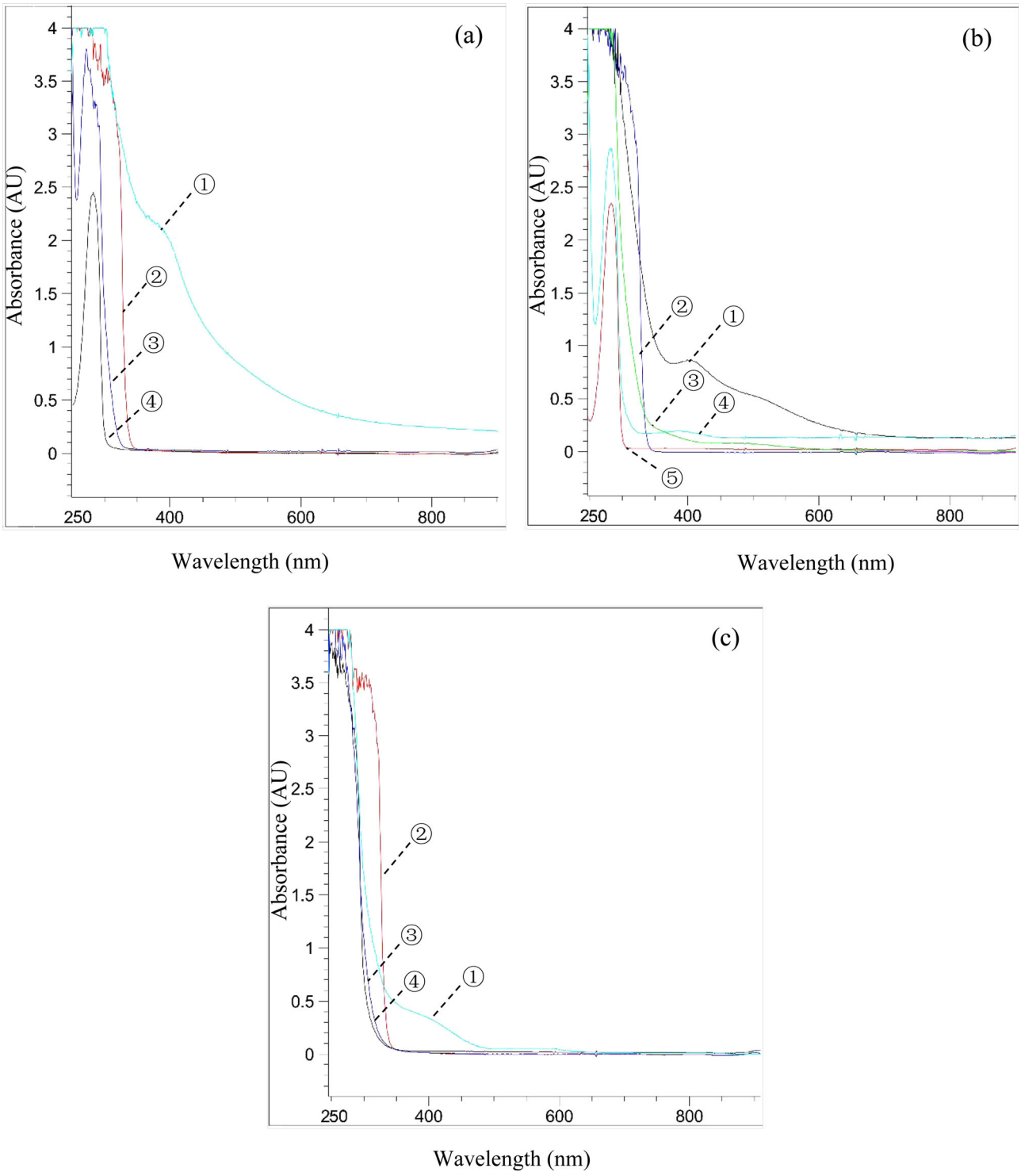

Figure 1. The effects of different solvents (e.g. aqueous buffer solution at pH 5.0 ①, ethyl acetate ②, acetone ③ and methanol ④) on the polymer products for 1.0 h by laccase (a), tyrosinase (b) or horseradish peroxidase (c) were investigated. Hydroxytyrosol ⑤ was used as a reference compared with the polymer in the UV-Vis scanning test. The other operation conditions were fixed as the following: reaction temperature 30 °C, hydroxytyrosol solution 5.0 mM and enzyme concentrations 8.0 μmol/L.

reddish-brown are reasonable due to a concentrated π–π structure and benzoquinones intermediate formation in the process of enzymatic polymerization. Nonetheless, those using methanol, acetone and ethyl acetate as a dissolving solvent were completely unchanged whatever of UV-Visible absorbance or the solution color. Similar findings could be observed by the preliminary work that the enzymatic oxidative polymerization of rutin performed the best in water (reaching 29-fold higher production), compared with acetonitrile, dimethylformamide, methanol, ethanol, acetone and tetrahydrofurane (Anthoni et al., 2008). Differences in the hydrophobicity and dielectric constant of the medium led to variations in the free energies of substrate–enzyme and substrate–solvent binding and hence, the enzyme's ability to make use of the free energy of binding to form the substrate-active site complex might be diminished (Rueda et al.,

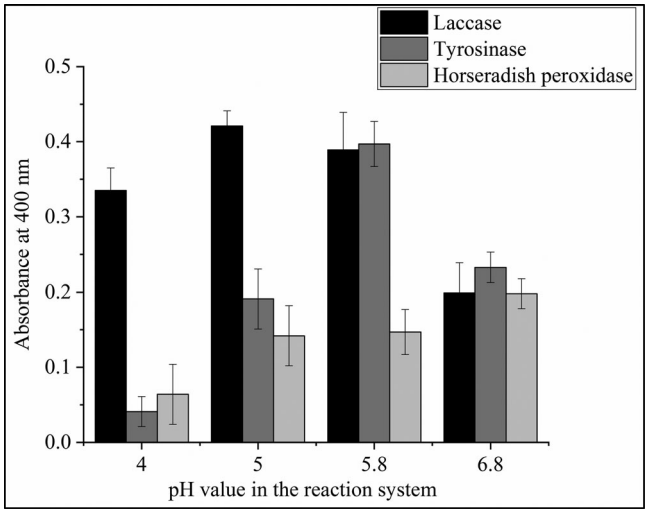

Figure 2. The effects of different pH values (4.0, 5.0, 5.8 and 6.8) on the polymer products for 1.0 h by laccase, tyrosinase or horseradish peroxidase were investigated. The other operation conditions were fixed as the following: reaction temperature 30 °C, hydroxytyrosol solution 5.0 mM and enzyme concentrations 8.0 μmol/L.

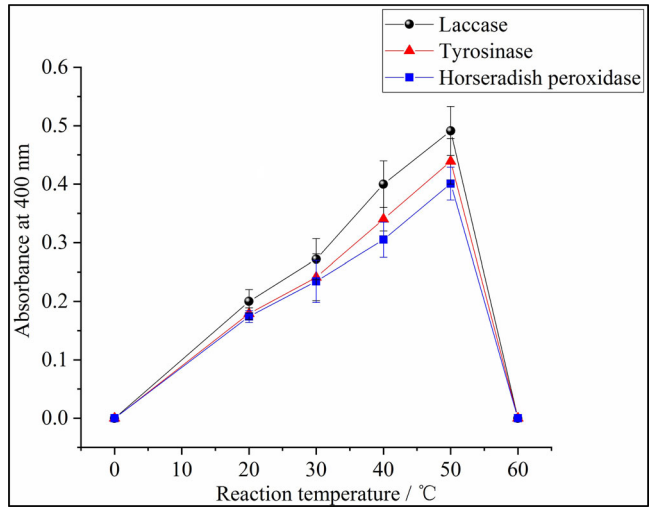

Figure 3. The effects of different reaction temperatures ranging from 30 to 60 °C on the polymer products by laccase, tyrosinase or horseradish peroxidase. The other operation conditions such as 30 min of reaction time, aqueous buffer solution (pH 5.0) and the ratio between these enzymes (8 μM) and hydroxytyrosol (5 mM) in molar were fixed.

2016). These implied that hydration of the enzyme was essential for activity. The presence of water in an organic-based biocatalytic system is now accepted as a prerequisite for enzyme activity since hydration facilitates the conformational flexibility necessary for catalysis by the protein (Hanoian et al., 2015). In organic solvent, the activity of oxidoreductases was reduced due to their denaturation in such environment (Rodakiewicz-Nowak, 2000). For that, the use of aqueous solvents was more suitable than organic one which affected drastically the yield, the solubility and the average molecular weight of obtained polymers, because of decreasing the enzyme affinity to the substrate in the hydrophobic solvent (Ikeda et al., 1998).

3.1.2. Selection of pH

Figure 2 indicated that laccase performed the best at pH 5.0 in the oxidative polymerization of hydroxytyrosol, and the suitable pH values in tyrosinase and horseradish peroxidase catalysis were showed at pH 5.8 and 5.0, respectively. These results were well matched with the previous findings that laccases' catalyzing function was stable pH ranging from 3.0 to 9.0 (Robles et al., 2000). Also, it was hardly affected the enzymatic polymerization at pH 8.0 and pH 9.0 for laccase, tyrosinase or horseradish peroxidase (data not shown). This agreed with the optimal conditions at pH 6.0 and 30 °C determined by the enzymes in mature coffee beans (Mazzafera & Robinson, 2000). Fungal laccases typically exhibit the optimal pH ranging from 3.5 to 5.0 when the substrates are hydrogen atom donor compound, and the pH-dependence curve is bell-shaped (Kurniawati & Nicell, 2008). Those pH ranges do not correspond to the optimal conversion microenvironment during the enzymatic polymerization. Indeed, it was reported that in the presence of laccase from *Trametes versicolor*, the best conversion yield (60%) was obtained at pH 5, while the optimal pH of this enzyme is from 6 to 8 (Kim & Nicell, 2006). Nevertheless, this influence was variable according to the used reactional media, showing that pH affected the type of linkage between monomeric units. An acid pH promoted the C–C linkage while C–O linkage was abundant at basic pH (Kobayashi et al., 1996). The effects of pH level ranging from 3 to 12 on polymerization of phenol by horseradish peroxidase or laccase indicating the yield and molecular weight almost presented a similar trend (Ikeda et al., 1998).

3.1.3. Selection of reaction temperature

Figure 3 indicated that the absorbance of hydroxytyrosol polymer at 400 nm gradually increased ranging from 30 to 50 °C by these enzymes. However, the continuing increase of hydroxytyrosol polymer content did not happen after 50 °C. The highest conversion yield resulted from laccase catalysis for the greatest decrease of hydroxytyrosol. Previous literature showed the optimized temperature for laccase-catalyzed polymerization typically ranged from 50 to 70 °C (Baldrian, 2004). There were few fungal laccases with an optimal oxidative profile below 35 °C (Koroleva et al., 2001). Reaction temperature can affect laccases activity, conversion rate, stability and solubility of phenols (Güreşir et al., 2005). This effect level was dependent on substrate and enzyme such as horseradish peroxidase when the enzymatic polymerization was executed ranging from 10 to 60 °C (González-Sánchez et al., 2011). High yields of polymerization (80%) were obtained as the temperature was inferior to 40 °C whereas the yield decreased by 31% at 60 °C owing to the thermal deactivation of the apo-protein. This will produce a lower concentration of radical species, indicating that reaction temperature was independent of the origin of these enzymes. Additionally, an increased temperature was helpful for the synthesis of polymers before deactivation. A similar observation was found that the highest production of polymers was reached at 50 °C, when the solubility of rutin and the laccase activity was desired (Kurisawa et al., 2003). Therefore, 50°C of

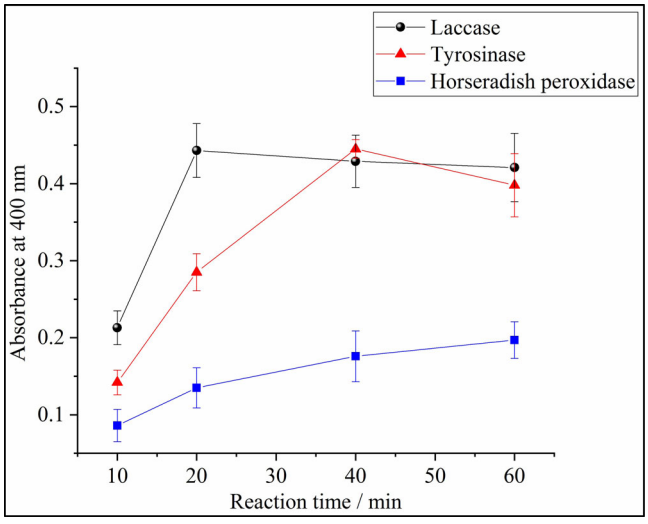

Figure 4. The effects of different times ranging from 10 to 60 min on the polymer products by laccase, tyrosinase or horseradish peroxidase. The other operation conditions such as 50 °C of reaction temperature, aqueous buffer solution (pH 5.0) and the ratio between these enzymes (8 μM) and hydroxytyrosol (5 mM) in molar were fixed.

the reaction temperature was the best choice as hydroxytyrosol oxidative polymerization for the three enzymes.

3.1.4 Selection of reaction time

Figure 4 indicated that the absorbance at 400 nm derived from hydroxytyrosol polymer and the polymer amounts significantly increased over time for the three enzymes, however, it only cost 20 min by laccase to achieve the maximal level, similar observations were found by tyrosinase and horseradish peroxidase but cost 40 min for a longer time. Besides, the absorbance of the resulting hydroxytyrosol polymer by laccase was 2.3-fold than that by horseradish peroxidase. Compared with tyrosinase, it cost less than 2-fold time by laccase to reach the same level of the hydroxytyrosol polymer. In monitoring the phenol conversion over time, it was apparent that the laccase had the highest rate of conversion (seen in Figure 4). Laccase was more efficient in oxidizing substrates with the predetermined enzyme concentrations. Horseradish peroxidases were quickly inactivated by the suicide mechanisms (resulting from phenoxy radicals) and/or by other inactivating mechanisms that may apply to the enzyme. Firstly, the highly reactive phenoxy radicals produced may react with the active site due to proximity, and alter its reactivity irreversibly. Secondly, the coupled products may adsorb the enzyme and coprecipitate it (Wu et al., 1998). Therefore, the suitable time for hydroxytyrosol oxidative polymerization catalyzed by laccase, tyrosinase or horseradish peroxidase were 20, 40 and 40 min in this study, respectively.

3.2. Docking and interaction between hydroxytyrosol and enzyme

As Figures 5(a) and S3 presented, laccase was checked by DS v4.0 and observed to have 24 cavities (sites) to be docked. Only six sites (site no. 3, 6, 9, 12, 14 and 19) were observed to have poses docked successfully. From Table S2, we found that hydroxytyrosol docking with site 9 was the best

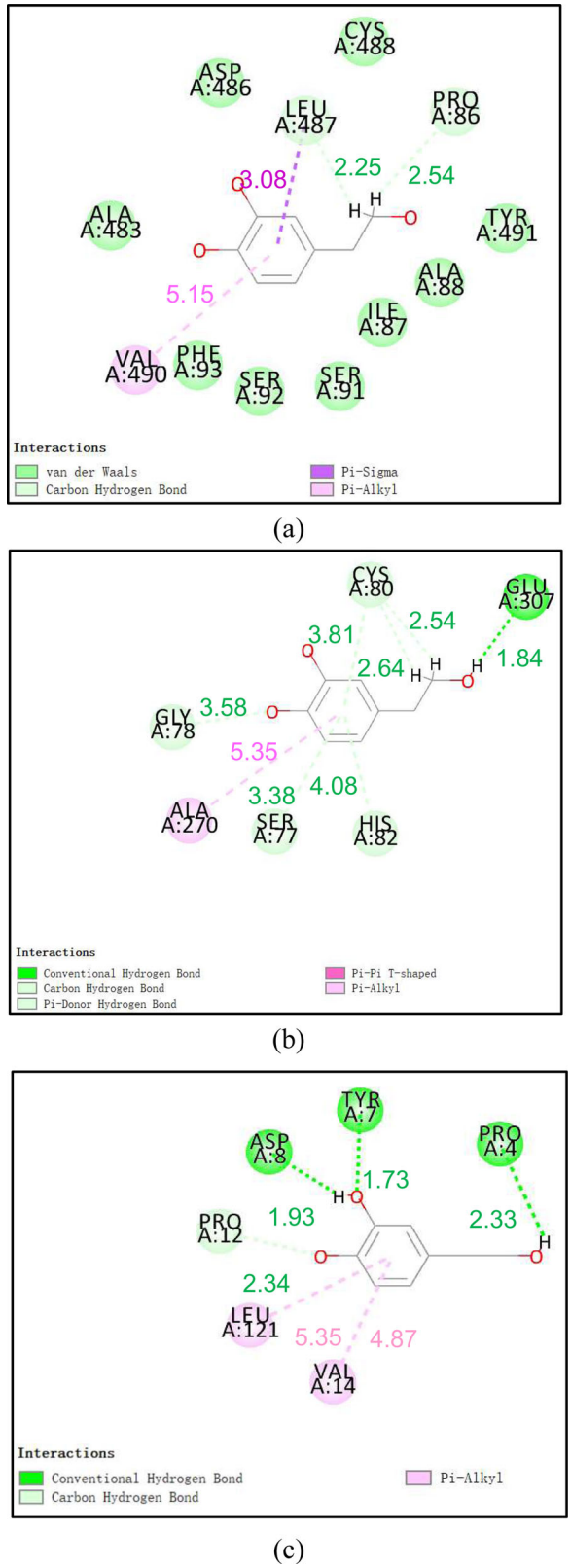

Figure 5. Docking results between HT and laccase in site 9 (a), tyrosinase in site 27 (b) and horseradish peroxidase in site 1 (c). The decoration of residues was expressed as blue background, hydrogen bond donor; red background, hydrogen bond acceptor; purple background, both hydrogen bond donor and acceptor; gray background, any other contact at all; and green background, nonpolar contact.

performance on the LibDockScore 75.91. To elucidate the interaction between hydroxytyrosol and laccase, tyrosinase or horseradish peroxidase, the docking simulation was carried out by MMFF forcefield and Libdock. Some parameters, such as conformation number, molecular number, pose number, absolute energy and relative energy were showed in Table S2 and Figure 5(a). The numbers of conformation, molecular, pose, absolute energy and relative energy in hydroxytyrosol were 1, 1, 1, 13.161 and $5.217e^{-15}$, respectively. Laccase providing the three donor atoms HG, H1 and H2 showed a strong interaction with the acceptor oxygen atom of hydroxytyrosol. Some details in different successful docking sites were further summarized in Table S2 and Figure S2(a). The major interactions between hydroxytyrosol and tyrosinase were driven by hydrogen bonding, Pi-Sigma, Pi-Alkyl and van der Waals' force. Taking site 9, for example (showed in Figures 5(a) and S3), three active interaction residue sites of laccase with hydroxytyrosol were PRO86, LEU487 and VAL490. Among them, PRO86 and LEU487 in laccase were hydrogen bond sites. The electron-donating group (peptide bond) from LEU487 bonded with an aromatic ring from hydroxytyrosol as a Pi-Sigma interacting played a key role in the oxidative polymerization process. The similar interaction between methyl from VAL490 and aromatic ring from hydroxytyrosol as Pi-Alkyl was found as well. The other residues contributing to hydrophobic interaction were given between ligands and receptors. van der Waals forces were found between carbon atom in ILE87, ALA88, SER91, SER92, PHE93, ALA483, ASP486, CYS488, TYR491 and H atom of hydroxyl in hydroxytyrosol ligand. This force offered strong energy to impact the spatial conformation of laccase. Since hydroxytyrosol could act on the residues of laccase, laccase activity was thus interfered or activated due to its change of structural conformation in the catalytic area (Mehra et al., 2018). Compared with the previous literatures, the interacting action types of our study were very similar including van der Waals, carbon hydrogen bond, Pi–Sigma and Pi–Alkyl. However, Pi–Pi T-shape and hydrogen bond are not included in our study on hydroxytyrosol docking with laccase, which could be possibly due to the different substrates (hydroxytyrosol and coumarins) and binding sites of the docking amino acids. The conformation of the active site was the key factor for laccase activity. A proper binding affinity for substrate–enzyme complex, and additional features in regard to the electron transfer was the best performance on enzymatic-catalyzing efficacy (Mehra et al., 2018). For instance, the suitable interaction between binding site of the laccase and hydroxytyrosol was better behavior than the substance with a strong hydrogen-binding. Moreover, the interactions between methyl caffeate and laccase consist of the hydrogen bonds (Gln237, Gln242, ILE236 and Val426 binding with carbonyl group, and Glu302, Ala410 binding with phenolic-hydroxyl groups) and van der Waals, etc. were obviously found (Conceição et al., 2020). Overall, these interactions contributed to the lowest (better) interaction energy in the case of this complex (Hongyan et al., 2019; Mo et al., 2018), were more superior enzyme-catalyzing efficacy than their highest (worse) interaction energy such as the laccase–methyl *p*-coumarate complex.

As observed in Figures 5(b), S2(b) and S4 showed that tyrosinase had 32 sites (cavity), but only successful docking site (1, 2, 5, 8, 11, 14, 15, 17, 22, 27 and 29) poses were produced. One of the best docking at site 27 indicated the highest scores 77.63 (seen in Table S3). Conventional hydrogen bond, pi–donor hydrogen bond, pi–pi T-shape, carbon–hydrogen bond and pi–alkyl were indicated as well. SER77, GLY78, CYS80, HIS82, ALA270 and GLU307 in tyrosinase were found to interact with hydroxytyrosol. The nitrogen atom in GLU307 with H atom of alcoholic hydroxyl in hydroxytyrosol produced a conventional hydrogen bond. Nevertheless, Carbon in CYS80 interacting with two H atoms of methylene in hydroxytyrosol formed a carbon-hydrogen bond. SER77, GLY78, CYS80 and HIS82 interacting with an aromatic ring in hydroxytyrosol were involved in a pi–donor hydrogen bond. Pi–pi T-shape interaction was formed by Pi from the double bond in ALA270 and pi from benzene ring in hydroxytyrosol, while pi–alkyl interaction was coming from Pi bond of the benzene ring in hydroxytyrosol and methyl in ALA270. Meanwhile, the different bonding distances were exhibited in Figure 5(b). To some extent, the distance implied a strong or weak interaction. In this case, the conventional hydrogen bond with the shortest distance of 1.84 Å was the strongest of all the interaction types. Tyrosinase so-called 'suicide enzyme' would be inactivated owing to the inside histidine destruction attacked by hydroxyl radicals, giving the peroxide-bridged enzyme intermediate by the incomplete reduction (Khan & Ali, 1986). Hence, irreversible inactivation of tyrosinase was attributed to the partial denaturation resulting from the disruption of intramolecular interactions by free radicals (Yang et al., 2015). Compared with previous literature concerning ferulic acid, cinnamic acid and quercetin docking with tyrosine, hydrogen bonds were produced by the different enzyme residues (Yu et al., 2019). Among them, one hydrogen-bond between the cinnamic acid and the residue Asn-22 (bond length: 2.3 Å), two hydrogen-bond interactions between the quercetin and the residues Asn-260 (bond length: 2.4 Å) and Met-280 (bond length: 1.8 Å) were observed. Also, two hydrogen-bond interactions between the ferulic acid and the residues Gln-307 (bond length: 2.1 Å) and Thr-308 (bond length: 1.9 Å) were yielded. As for the hydrophobic area, Pi-cation/anion interaction between them (ferulic acid: cation-Pi Lys-376 and anion–π interactions with the residues Asp-312 and Glu-356; quercetin: CH–π interaction with the residue Phe-264). However, our result was related to producing one hydrogen-bond from the interaction between HT(H) and GLU307. The hydrophobic interactions such as pi–pi T-shape, carbon–hydrogen bond and pi–alkyl were found as well in our study. Overall, all these interactions helped these phenolic compounds containing *o*-dihydroxyl group to anchor in the binding site of tyrosinase.

Figure 5(c) illustrated a successful docking with a Libdock technique between hydroxytyrosol and horseradish peroxidase. Nine sites could be successfully observed from horseradish peroxidase. Among others, only sites 1, 3, 6 and 7 were successfully generated, as shown in Figures S2(c) and S5. The

best docking site in horseradish peroxidase for hydroxytyrosol showed site 1 acquiring the highest docking scores 86.09 (seen in Table S4). Conventional hydrogen bond, carbon–hydrogen bond and pi–alkyl interactions were found and the specific amino acids were involved in PRO4, TYR7, ASP8, PRO12, LEU121 and VAL14. Furthermore, conventional hydrogen bonds (green color) resulted from H atom in hydroxytyrosol and N atom in PRO4 and ASP8, and O atom in hydroxytyrosol and H atom in TYR7. Hydrogen bond (light green color) was produced from O atom in hydroxytyrosol and H atom in PRO12. Pi–alkyl interaction was produced from an aromatic ring and methyl group in LEU121 and VAL14. From the bond length, conventional hydrogen bond with the shortest distance 1.73 Å played the key role in impacting the spatial structure of horseradish peroxidase which thus possibly resulted in a different catalyzing process. This was in good agreement with the behavior referred as the suicide inactivation of horseradish peroxidase by H_2O_2 (Garcia-Molina et al., 2005). As previous literatures indicated, hydrogen bonds are found between two phenolic H atoms of coumarins and N atom of catalytic residue HIS42, and O atom of H_2O; between one phenolic O atom of coumarins and H atom of the residue ARG38. The hydrogen bonding network with HIS42, ARG38 and the distal water molecule makes the extended interaction between coumarin and horseradish peroxidase. For coumarins containing dihydroxyls, both hydroxyl groups could form hydrogen bonds with HIS42 in the horseradish peroxidase (Gao et al., 2016). Amino acid residues of the horseradish peroxidase with apigenin also produced hydrogen bonding, including ARG31, ALA34, SER35, ARG38, PRO141, LYS174 and PHE221 with their relevant hydroxyl groups of apigenin (Mahfoudi et al., 2017). The phenolic substrate was much closer to the binding area of horseradish peroxidase suggesting an easier to produce strong hydrogen bond, which was not beneficial to improve the enzyme-catalyzing efficacy (Yan et al., 2019), as our findings indicated.

3.3. MD simulations

MD simulations were used to verify the complexes formed by HT and laccase in site 9, HT and tyrosinase in site 27 and HT and horseradish peroxidase in site 1, as indicated in Figures S3–S5. The 224 *ps* MD simulations initialized from the laccase-hydroxytyrosol, tyrosinase-hydroxytyrosol and horseradish-peroxidase-hydroxytyrosol complexes from docking and their structures were studied. The time evolutions of RMSD of hydroxytyrosol were shown in Figure 6. The RMSD against simulation time was helpful to estimate the equilibration procedure in the simulation trajectory and the structural stability when these enzymes were bond with a ligand of hydroxytyrosol (Awasthi et al., 2015). The simulated results from Figure 6(a–c) indicated that the laccase-hydroxytyrosol complex in 152 *ps*, tyrosinase-hydroxytyrosol complex in 175 *ps* and horseradish-peroxidase-hydroxytyrosol complex in 150 *ps* achieved equilibrium. Therefore, 100 structure models from the last 49 *ps* were chosen. The achieved level of the equilibrium represented by the RMSD for the laccase-hydroxytyrosol, tyrosinase-hydroxytyrosol and horseradish-peroxidase-hydroxytyrosol were 1.50, 1.31 and 1.10, accordingly. The reduction of RMSD in the complex comparable to the stability of the enzyme was elevated upon the different bindings of hydroxytyrosol. Because the complex size was the key factor, the more compact of the HT-enzyme complex resulted from a synergic conformation change intimately accessibility with hydroxytyrosol. Likewise, the RMSF for the laccase-hydroxytyrosol, tyrosinase-hydroxytyrosol and horseradish-peroxidase-hydroxytyrosol varied significantly. The increased level of the complex size indicated the more flexible. In this scenario, laccase-hydroxytyrosol complex performed the best, followed by horseradish-peroxidase-hydroxytyrosol and tyrosinase-hydroxytyrosol, as observed in Figure 6. The average solvent accessible surface area to laccase-hydroxytyrosol, tyrosinase-hydroxytyrosol and horseradish-peroxidase-hydroxytyrosol were getting bigger and bigger by order. It further confirmed that these enzymes had conformational changes at given regions to facilitate the interaction with hydroxytyrosol, and thoroughly flexible MD simulation was indispensable to inspect ligand binding to protein over semi-flexible molecular docking. Because of the evidenced hydroxylation activity of enzyme toward its natural substrate in combination with the consistent proposed novel reaction mechanism, another complexion was put on the function of polyphenol oxidases (Molitor et al., 2016). From Figures 6(a) and S6(a), the time in maintaining equilibrium between 120 and 175 *ps* of simulation were perceived. All the further analysis during this equilibrium elucidated that the docked enzymatic protein had achieved compactness.

Interactive energy changes of molecular dynamics between hydroxytyrosol and laccase, tyrosinase or horseradish peroxidase, were seen in Table S4. For the laccase–hydroxytyrosol complex, the initial potential energy (kcal/mol) was decreased from 2.09×10^7 to 1.19×10^5 during 152 *ps*. Kinetic energy (kcal/mol) increasing from 22485 to 23306 and van der Waals energy (kcal/mol) from 1020 increasing to 4434 was achieved when the temperature reached 300.4 K. In this period, electrostatic energy had almost no change. To sum up, the total energy (kcal/mol) was decreased from -9.70×10^4 to -9.87×10^4. Likewise, from Figures 6(b) and S6(b), the initial potential energy (kcal/mol) of the tyrosinase-hydroxytyrosol complex was decreased from 2.70×10^6 to −93,411 during 15 *ps*. Kinetic energy (kcal/mol) decreasing from 11,240 to 11,203 (almost no change), van der Waals energy (kcal/mol) increasing from −7312 to −5894.838 were achieved when the temperature was heated to 299.4 K. In this period, electrostatic energy changed from −52,799.12 to −72,515.2. In this manner, the total energy (kcal/mol) was decreased from -4.59×10^4 to -4.96×10^4 from Figures 6(c) and S6(c), the initial potential energy (kcal/mol) of the horseradish-peroxidase-hydroxytyrosol complex decreasing from 9.83×10^{13} to −93,411 during 15 *ps*. Kinetic energy (kcal/mol) increasing from 16,867 to 17,401 and van der Waals energy (kcal/mol) increasing from 1784 to 4331 were achieved when the temperature was increased to 307.4 K. In this period, electrostatic energy had little change from

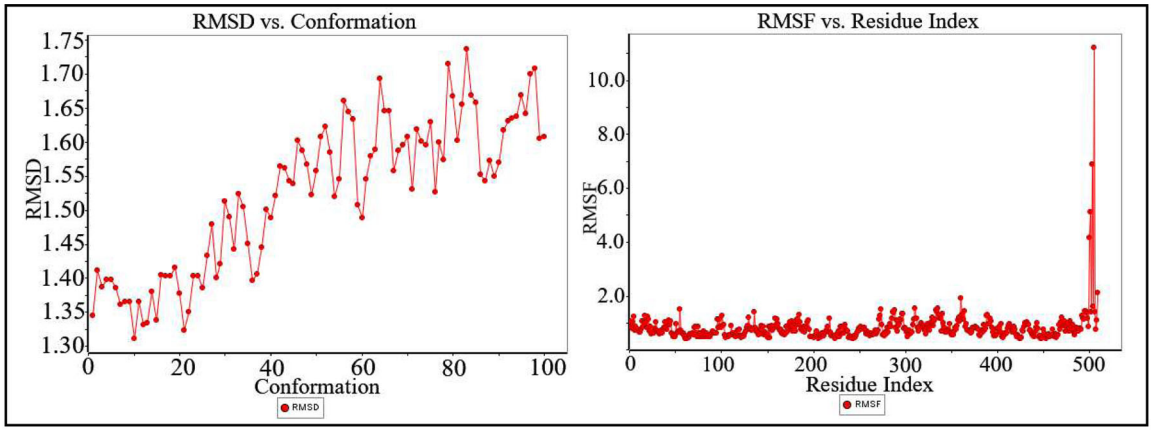

(a)

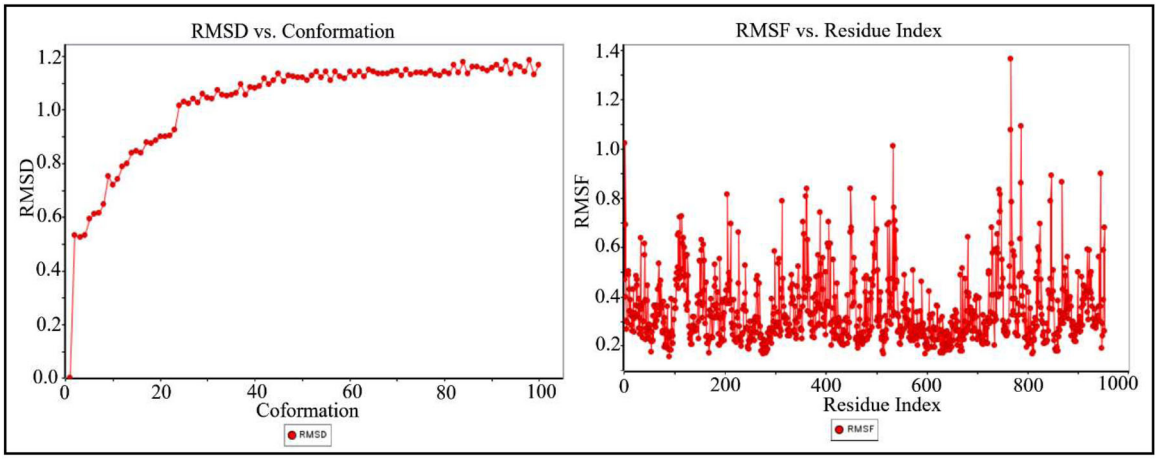

(b)

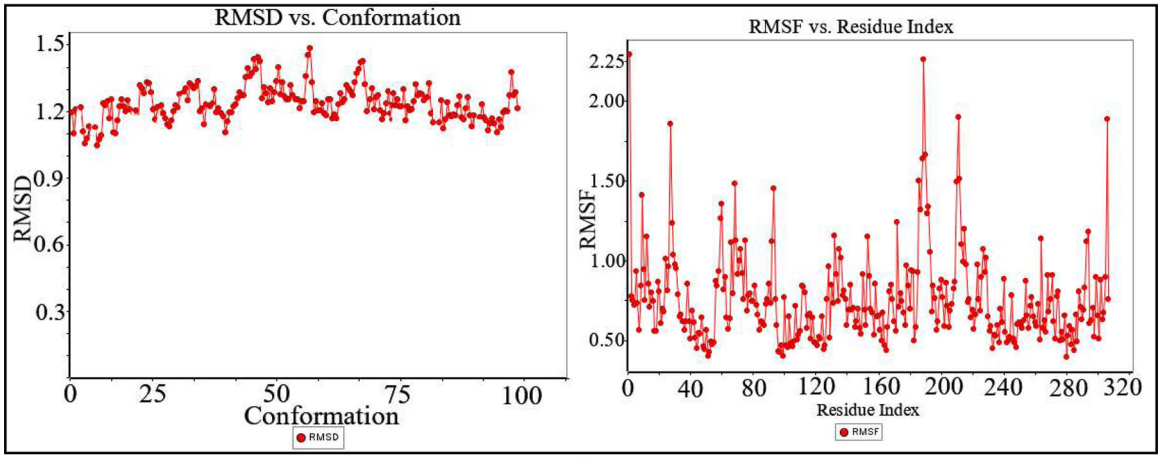

(c)

Figure 6. Molecular dynamics by the complexes: HT-laccase (a), HT-tyrosinase (b) and HT-horseradish peroxidase (c). LAC, laccase; TYR, tyrosinase; and HRP, horseradish peroxidase were presented.

−81,728.6 to −81,930. The total energy (kcal/mol) decreasing from -7.59×10^4 to -7.68×10^4 was indicated. Overall, all these energy variations were closely related to catalyzing efficacy for these enzymes.

3.4. Torsion analysis of hydroxytyrosol

As Table S5 indicated, compared with torsion of free hydroxytyrosol, There are 46 torsion angles produced based on the chemical structure of hydroxytyrosol (HT), however, only 19 torsion angles (Table S6) from 5 backbones (C1–O7, C2–O8, C5–C9, C9–C10 and C10-O11) rotation ($\varphi_1 \sim \varphi_5$, seen in Figure S6) gave a relative high variation compared with these angels in free hydroxytyrosol. For φ_1 and φ_2, formed by the rotation of C1–O7 and C2–O8 in phenolic hydroxyl of the HT, all the enzymes (laccase, tyrosinase and horseradish peroxidase) performed the similar action, can induce the C–O to rotate when binding with HT in different interactions acting as a biocatalyst. Rotating by 53.3° from 2.9° or −177.2

to 56.2° or 123.8° for the HT binding with the three enzymes, compared with free HT, achieved the best match with these enzymes in geometry and energy (Bruno et al., 2010). For φ_3, formed by rotation of backbone (C5–C9), on one hand, HT binding with the different enzymes gave a different levels on rotation. C4 (C6)–C5–C9–C10 as backbone chain was impacted by the binding tyrosinase more than that by laccase (20°) or horseradish peroxidase (22°), their absolute values of the torsion angles variation for binding tyrosinase reached 48° to possibly lower steric hindrance effect (Chen et al., 2017; Dicésare et al., 1999). On the other hand, C4 (C6)–C5–C9–H17 as backbone chain was impacted by the laccase more than that by tyrosinase or horseradish peroxidase, their absolute values of the torsion angles variation for binding tyrosinase reached 108° possibly due to the flexibility of the lighter H atom. The torsion variation of C4 (C6)–C5–C9–H18 was similar to the observations of C4 (C6)–C5–C9–H17 but the absolute value was 126°. For φ_4, C5–C9 (H17)–C10–O11(H20) as backbone chain induced by horseradish peroxidase reached 105° and 109°, which was obviously greater than that was almost kept unchanged by laccase and tyrosinase. Likewise, H17(H18)–C9–C10–H19(H20) in HT as backbone chain induced by laccase rotated over 110° more than that by tyrosinase and horseradish peroxidase, indicating that the relevant H atoms were easier to rotate by laccase (Mezei & Csonka, 2015). For φ_5, the torsion of H19 (H20)–C10–O11–H21 by horseradish peroxidase were changed over 118° in average more than that almost kept unchanged by laccase and tyrosinase.

Furthermore, as Table S7 showed, compared with the bonds of free hydroxytyrosol (initial status), the bond lengths of hydroxytyrosol (final status) binding with laccase, tyrosinase or horseradish peroxidase gave a varying degree depending on the specific enzyme and bonded atoms. For the hydroxytyrosol at final status, the bond lengths from binding laccase changed the most reaching 30% longer increased in total (the sum of all the bonds lengths in hydroxytyrosol), whereas the other two hydroxytyrosol bond lengths from binding enzymes almost kept unchanged. That means hydroxytyrosol was possibly activated by binding laccase due to getting the bond lengths longer (Cambria et al., 2012; Pogni et al., 2015). Particularly, all the lengths between O and H in the hydroxyl groups of the hydroxytyrosol were obviously getting longer reaching over 10% and thus easier to get broken and further conduct ensuing self-polymerization reaction for *o*-phenolic hydroxyl groups (O7–H15 and O8–H16). That's well matched with our experiments' results that laccase catalysis performed the best on hydroxytyrosol polymerization.

4. Conclusions

The oxidative polymerization of hydroxytyrosol catalyzed by laccase, tyrosinase or horseradish peroxidase was proved to be a feasible transformation way. Hydroxytyrosol polymerization by laccase showed the best performance under reaction temperature 50°C for 20 min in a buffer aqueous solution of pH 5.0. The main driving forces of hydrogen bonding, pi–sigma, pi–alkyl and van der Waals' force interactions were critical for the catalysis process and enzyme change. Specifically, PRO4, TYR7, ASP8, PRO12, LEU121 and VAL14 in laccase interacted with hydroxytyrosol. The time of achieving interaction balance goes within 175 ps. Structural analysis in view of torsion and bond lengths showed that the C–O of phenolic bonds from hydroxytyrosol gave an obvious rotation and its length of the related O–H became longer when binding to laccase compared with free hydroxytyrosol. These findings are gainful to deeply understand the enzymatic polymerization process of the catechin-based phenolics with the catalysis of oxidoreductase. In addition, this study might provide an innovative pathway with oxidoreductase to disposing the olive by-products such as olive mill wastewater or olive pomace in a green and environmentally friendly sense and obtaining highly value-added oligomers.

Acknowledgements

We thanked the computational support of *Discovery Studio v4.0* from Prof. Qiu Minghua in Kunming Institute of Botany, Chinese Academy of Sciences.

Disclosure statement

No potential conflict of interest was reported by the authors.

Funding

Funding support of this study was derived from Fundamental Research Funds of CAF (grant no. CAFYBB2020SY036), Natural Science Foundation of China (grant no. 31800614) and Jiangsu Provincial Natural Science Foundation of China (grant no. BK20181124).

ORCID

Lixin Huang https://orcid.org/0000-0002-8507-1910

References

Anthoni, J., Lionneton, F., Wieruszeski, J. M., Magdalou, J., Engasser, J. M., Chebil, L., Humeau, C., & Ghoul, M. (2008). Investigation of enzymatic oligomerization of rutin. *Rasayan Journal of Chemistry*, *1*, 718–731.

Araújo, M., Pimentel, F. B., Alves, R. C., & Oliveira, M. B. P. P. (2015). Phenolic compounds from olive mill wastes: Health effects, analytical approach and application as food antioxidants. *Trends in Food Science & Technology*, *45*(2), 200–211. https://doi.org/10.1016/j.tifs.2015.06.010

Awasthi, M., Jaiswal, N., Singh, S., Pandey, V. P., & Dwivedi, U. N. (2015). Molecular docking and dynamics simulation analyses unraveling the differential enzymatic catalysis by plant and fungal laccases with respect to lignin biosynthesis and degradation. *Journal of Biomolecular Structure & Dynamics*, *33*(9), 1835–1849. https://doi.org/10.1080/07391102.2014.975282

Baldrian, P. (2004). Purification and characterization of laccase from the white-rot fungus *Daedalea quercina* and decolorization of synthetic dyes by the enzyme. *Applied Microbiology and Biotechnology*, *63*(5), 560–563. https://doi.org/10.1007/s00253-003-1434-0

Bilal, M., Adeel, M., Rasheed, T., Zhao, Y., & Iqbal, H. M. N. (2019). Emerging contaminants of high concern and their enzyme-assisted biodegradation—A review. *Environment International*, *124*, 336–353. https://doi.org/10.1016/j.envint.2019.01.011

Bruno, F. F., Trotta, A., Fossey, S., Nagarajan, S., Nagarajan, R., Samuelson, L. A., & Kumar, J. (2010). Enzymatic synthesis and characterization of polyquercetin. *Journal of Macromolecular Science, Part A*, *47*(12), 1191–1196. https://doi.org/10.1080/10601325.2010.518839

Cambria, M. T., Gullotto, D., Garavaglia, S., & Cambria, A. (2012). In silico study of structural determinants modulating the redox potential of *Rigidoporus lignosus* and other fungal laccases. *Journal of Biomolecular Structure & Dynamics*, *30*(1), 89–101. https://doi.org/10.1080/07391102.2012.674275

Cardinali, A., Cicco, N., Linsalata, V., Minervini, F., Pati, S., Pieralice, M., Tursi, N., & Lattanzio, V. (2010). Biological activity of high molecular weight phenolics from olive mill wastewater. *Journal of Agricultural and Food Chemistry*, *58*(15), 8585–8590. https://doi.org/10.1021/jf101437c

Chen, Y., Zhao, L., & Jiang, J. (2017). The naphthoate-modifying Cu^{2+}-detective Bodipy sensors with the fluorescent ON-OFF performance unaffected by molecular configuration. *Spectrochimica Acta. Part A, Molecular and Biomolecular Spectroscopy*, *175*, 269–275. https://doi.org/10.1016/j.saa.2016.12.034

Conceição, J. C. S., Dias, H. J., Peralva, C. M. S., Crotti, A. E. M., da Rocha Pita, S. S., & de Oliveira Silva, E. (2020). Phenolic compound biotransformation by *Trametes versicolor ATCC 200801* and molecular docking studies. *Applied Biochemistry and Biotechnology*, *190*(4), 1498–1511. https://doi.org/10.1007/s12010-019-03191-y

Dec, J., & Bollag, J. M. (1990). Detoxification of substituted phenols by oxidoreductive enzymes through polymerization reactions. *Archives of Environmental Contamination and Toxicology*, *19*(4), 543–550. https://doi.org/10.1007/BF01059073

Desentis-Mendoza, R. M., Hernández-Sánchez, H., Moreno, A., Rojas del C, E., Chel-Guerrero, L., Tamariz, J., & Jaramillo-Flores, M. E. (2006). Enzymatic polymerization of phenolic compounds using laccase and tyrosinase from *Ustilago maydis*. *Biomacromolecules*, *7*(6), 1845–1854. https://doi.org/10.1021/bm060159p

Dicésare, N., Belletête, M., Leclerc, M., & Durocher, G. (1999). HF/3-21G* ab initio calculations on methoxy-substituted bithiophenes. *Journal of Molecular Structure: Theochem*, *467*(3), 259–273. https://doi.org/10.1016/S0166-1280(99)00002-0

Duran, N., & Esposito, E. (2000). Potential applications of oxidative enzymes and phenoloxidase-like compounds in wastewater and soil treatment: A review. *Applied Catalysis B: Environmental*, *28*(2), 83–99. https://doi.org/10.1016/S0926-3373(00)00168-5

Edwards, W., Bownes, R., Leukes, W. D., Jacobs, E. P., Sanderson, R., Rose, P. D., & Burton, S. G. (1999). A capillary membrane bioreactor using immobilized polyphenol oxidase for the removal of phenols from industrial effluents. *Enzyme and Microbial Technology*, *24*(3–4), 209–217. https://doi.org/10.1016/S0141-0229(98)00110-0

Gao, X., Huang, S., Dong, P., Wang, C., Hou, J., Huo, X., Zhang, B., Ma, T., & Ma, X. (2016). Horseradish peroxidase (HRP): A tool for catalyzing the formation of novel bicoumarins. *Catalysis Science & Technology*, *6*(10), 3585–3593. https://doi.org/10.1039/C5CY01682G

Garcia-Molina, F., Hiner, A. N. P., Fenoll, L. G., Rodriguez-Lopez, J. N., Garcia-Ruiz, P. A., Garcia-Canovas, F., & Tudela, J. (2005). Mushroom tyrosinase: Catalase activity, inhibition, and suicide inactivation. *Journal of Agricultural and Food Chemistry*, *53*(9), 3702–3709. https://doi.org/10.1021/jf048340h

González-Sánchez, M. I., Laurenti, M., Rubio-Retama, J., Valero, E., & Lopez-Cabarcos, E. (2011). Fluorescence decrease of conjugated polymers by the catalytic activity of horseradish peroxidase and its application in phenolic compounds detection. *Biomacromolecules*, *12*(4), 1332–1338. https://doi.org/10.1021/bm200091m

Güreşir, M., Aktaş, N., & Tanyolaç, A. (2005). Influence of reaction conditions on the rate of enzymic polymerization of pyrogallol using laccase. *Process Biochemistry*, *40*(3–4), 1175–1182. https://doi.org/10.1016/j.procbio.2004.04.007

Hanoian, P., Liu, C. T., Hammes-Schiffer, S., & Benkovic, S. (2015). Perspectives on electrostatics and conformational motions in enzyme catalysis. *Accounts of Chemical Research*, *48*(2), 482–489. https://doi.org/10.1021/ar500390e

Hongyan, L., Zexiong, Z., Shiwei, X., He, X., Yinian, Z., Haiyun, L., & Zhongsheng, Y. (2019). Study on transformation and degradation of bisphenol A by *Trametes versicolor* laccase and simulation of molecular docking. *Chemosphere*, *224*, 743–750. https://doi.org/10.1016/j.chemosphere.2019.02.143

Hosny, M., & Rosazza, J. P. N. (2002). Novel oxidations of (+)-catechin by horseradish peroxidase and laccase. *Journal of Agricultural and Food Chemistry*, *50*(20), 5539–5545. https://doi.org/10.1021/jf020503j

Ikeda, R., Sugihara, J., Uyama, H., & Kobayashi, S. (1998). Enzymatic oxidative polymerization of 4-hydroxybenzoic acid derivatives to poly(phenylene oxide)s. *Polymer International*, *47*(3), 295–301. https://doi.org/10.1002/(SICI)1097-0126(199811)47:3<295::AID-PI7>3.0.CO;2-W

Ikehata, K., & Nicell, J. A. (2000). Characterization of tyrosinase for the treatment of aqueous phenols. *Bioresource Technology*, *74*(3), 191–199. https://doi.org/10.1016/S0960-8524(00)00025-0

Khan, I. A., & Ali, R. (1986). Antigenicity, catalytic activity and conformation of Agaricus bisporus tyrosinase: interaction of conformation-directed antibodies with the native and irradiated enzyme . *Journal of Biochemistry*, *99*(2), 445–452. https://doi.org/10.1093/oxfordjournals.jbchem.a135498

Kim, Y. J., & Nicell, J. A. (2006). Impact of reaction conditions on the laccase-catalyzed conversion of bisphenol A. *Bioresource Technology*, *97*(12), 1431–1442. https://doi.org/10.1016/j.biortech.2005.06.017

Kobayashi, S., Kurioka, H., & Uyama, H. (1996). Enzymatic synthesis of a soluble polyphenol derivative from 4,4′-biphenyldiol. *Macromolecular Rapid Communications*, *17*(8), 503–508. https://doi.org/10.1002/marc.1996.030170802

Kobayashi, S., Uyama, H., & Kimura, S. (2001). Enzymatic polymerization. *Chemical Reviews*, *101*(12), 3793–3818. https://doi.org/10.1021/cr990121l

Koroleva, O. V., Gavrilova, V. P., Yavmetdinov, I. S., Shleev, S. V., & Stepanova, E. V. (2001). Isolation and study of some properties of laccase from the *Basidiomycetes Cerrena maxima*. *Biochemistry. Biokhimiia*, *66*(6), 618–622.

Kurisawa, M., Chung, J. E., Kim, Y. J., Uyama, H., & Kobayashi, S. (2003). Amplification of antioxidant activity and xanthine oxidase inhibition of catechin by enzymatic polymerization. *Biomacromolecules*, *4*(3), 469–471. https://doi.org/10.1021/bm034012z

Kurniawati, S., & Nicell, J. A. (2008). Characterization of *Trametes versicolor* laccase for the transformation of aqueous phenol. *Bioresource Technology*, *99*(16), 7825–7834. https://doi.org/10.1016/j.biortech.2008.01.084

Litescu, S. C., Eremia, S., & Radu, G. L. (2010). Biosensors for the determination of phenolic metabolites. *Advances in Experimental Medicine and Biology*, *698*, 234–240. https://doi.org/10.1007/978-1-4419-7347-4_17

Liu, W. Y., Zou, C. M., Hu, J. H., Xu, Z. J., Si, L. Q., Liu, J. J., & Huang, J. G. (2020). Kinetic characterization of tyrosinase-catalyzed oxidation of four polyphenols. *Current Medical Science*, *40*(2), 239–248. https://doi.org/10.1007/s11596-020-2186-0

Mahfoudi, R., Djeridane, A., Benarous, K., Gaydou, E. M., & Yousfi, M. (2017). Structure-activity relationships and molecular docking of thirteen synthesized flavonoids as horseradish peroxidase inhibitors. *Bioorganic Chemistry*, *74*, 201–211. https://doi.org/10.1016/j.bioorg.2017.08.001

Marszałek, K., Krzyżanowska, J., Woźniak, Ł., & Skąpska, S. (2017). Kinetic modelling of polyphenol oxidase, peroxidase, pectin esterase, polygalacturonase, degradation of the main pigments and polyphenols in beetroot juice during high pressure carbon dioxide treatment. *LWT—Food Science and Technology*, *85*, 412–417. https://doi.org/10.1016/j.lwt.2016.11.018

Mazzafera, P., & Robinson, S. P. (2000). Characterization of polyphenol oxidase in coffee. *Phytochemistry*, *55*(4), 285–296. https://doi.org/10.1016/S0031-9422(00)00332-0

Mehra, R., Muschiol, J., Meyer, A. S., & Kepp, K. P. (2018). A structural-chemical explanation of fungal laccase activity. *Scientific Report-UK*, *8*, 17285.

Mezei, P. D., & Csonka, G. I. (2015). Unified picture for the conformation and stabilization of the O-glycosidic linkage in glycopeptide model structures. *Structural Chemistry*, *26*(5–6), 1367–1376. https://doi.org/10.1007/s11224-015-0666-9

Mo, D., Zeng, G., Yuan, X., Chen, M., Hu, L., Li, H., Wang, H., Xu, P., Lai, C., Wan, J., Zhang, C., & Cheng, M. (2018). Molecular docking simulation on the interactions of laccase from *Trametes versicolor* with nonylphenol and octylphenol isomers. *Bioprocess and Biosystems Engineering*, *41*(3), 331–343. https://doi.org/10.1007/s00449-017-1866-z

Molitor, C., Mauracher, S. G., & Rompel, A. (2016). Aurone synthase is a catechol oxidase with hydroxylase activity and provides insights into the mechanism of plant polyphenol oxidases. *Proceedings of the National Academy of Sciences*, *113*(13), E1806–1815. https://doi.org/10.1073/pnas.1523575113

Oliver, S., Vittorio, O., Cirillo, G., & Boyer, C. (2016). Enhancing the therapeutic effects of polyphenols with macromolecules. *Polymer Chemistry*, *7*(8), 1529–1544. https://doi.org/10.1039/C5PY01912E

Paulo, F., & Santos, L. (2020). Deriving valorization of phenolic compounds from olive oil by-products for food applications through microencapsulation approaches: A comprehensive review. *Critical Reviews in Food Science and Nutrition*, *11*, 1–26.

Pinheiro, V. E., Michelin, M., Vici, A. C., de Almeida, P. Z., & Teixeira de Moraes Polizeli, MdL. (2020). *Trametes versicolor* laccase production using agricultural wastes: A comparative study in erlenmeyer flasks, bioreactor and tray. *Bioprocess and Biosystems Engineering*, *43*(3), 507–514. https://doi.org/10.1007/s00449-019-02245-z

Pogni, R., Baratto, M. C., Sinicropi, A., & Basosi, R. (2015). Spectroscopic and computational characterization of laccases and their substrate radical intermediates. *Cellular and Molecular Life Sciences*, *72*(5), 885–896. https://doi.org/10.1007/s00018-014-1825-7

Roberts, J. J., Naudiyal, P., Lim, K. S., Poole-Warren, L. A., & Martens, P. J. (2016). A comparative study of enzyme initiators for crosslinking phenol-functionalized hydrogels for cell encapsulation. *Biomaterials Research*, *20*, 30–42. https://doi.org/10.1186/s40824-016-0077-z

Robles, A., Lucas, R., de Cienfuegos, G. A., & Gálvez, A. (2000). Phenol-oxidase (laccase) activity in strains of the hyphomycete *Chalara paradoxa* isolated from olive mill wastewater disposal ponds. *Enzyme and Microbial Technology*, *26*, 484–490. https://doi.org/10.1016/S0141-0229(99)00197-0

Rodakiewicz-Nowak, J. (2000). Phenols oxidizing enzymes in water-restricted media. *Topics in Catalysis*, *11/12*(1/4), 419–434. https://doi.org/10.1023/A:1027291629302

Rueda, N., dos Santos, J. C. S., Ortiz, C., Torres, R., Barbosa, O., Rodrigues, R. C., Berenguer-Murcia, Á., & Fernandez-Lafuente, R. (2016). Chemical modification in the design of immobilized enzyme biocatalysts: Drawbacks and opportunities. *Chemical Record (New York, N.Y.)*, *16*(3), 1436–1455. https://doi.org/10.1002/tcr.201600007

Sánchez-Ferrer, Á., Neptuno Rodríguez-López, J., García-Cánovas, F., & García-Carmona, F. (1995). Tyrosinase: A comprehensive review of its mechanism. *Biochimica et Biophysica Acta (BBA)—Protein Structure and Molecular Enzymology*, *1247*(1), 1–11. https://doi.org/10.1016/0167-4838(94)00204-T

Sarkar, S., Banerjee, A., Chakraborty, N., Soren, K., Chakraborty, P., & Bandopadhyay, R. (2020). Structural-functional analyses of textile dye degrading azoreductase, laccase and peroxidase: A comparative in silico study. *Electronic Journal of Biotechnology*, *43*, 48–54. https://doi.org/10.1016/j.ejbt.2019.12.004

Shalit, H., Dyadyuk, A., & Pappo, D. (2019). Selective oxidative phenol coupling by iron catalysis. *The Journal of Organic Chemistry*, *84*(4), 1677–1686. https://doi.org/10.1021/acs.joc.8b03084

Shleev, S., Reimann, C. T., Serezhenkov, V., Burbaev, D., Yaropolov, A. I., Gorton, L., & Ruzgas, T. (2006). Autoreduction and aggregation of fungal laccase in solution phase: Possible correlation with a resting form of laccase. *Biochimie*, *88*(9), 1275–1285. https://doi.org/10.1016/j.biochi.2006.02.007

Shoda, S. I., Uyama, H., Kadokawa, J. I., Kimura, S., & Kobayashi, S. (2016). Enzymes as green catalysts for precision macromolecular synthesis. *Chemical Reviews*, *116*(4), 2307–2413. https://doi.org/10.1021/acs.chemrev.5b00472

Solná, R., & Skládal, P. (2005). Amperometric flow-injection determination of phenolic compounds using a biosensor with immobilized laccase, peroxidase and tyrosinase. *Electroanalysis*, *17*(23), 2137–2146. https://doi.org/10.1002/elan.200403343

Solomon, E. I., Augustine, A. J., & Yoon, J. (2008). O_2 Reduction to H_2O by the multicopper oxidases. *Dalton Transactions*, *30*(30), 3921–3932. https://doi.org/10.1039/b800799c

Stadlmair, L. F., Letzel, T., & Graßmann, J. (2018). Monitoring enzymatic degradation of emerging contaminants using a chip-based robotic nano-ESI-MS tool. *Analytical and Bioanalytical Chemistry*, *410*(1), 27–32. https://doi.org/10.1007/s00216-017-0729-4

Torres, E., Bustos-Jaimes, I., & Le Borgne, S. (2003). Potential use of oxidative enzymes for the detoxification of organic pollutants. *Applied Catalysis B: Environmental*, *46*(1), 1–15. https://doi.org/10.1016/S0926-3373(03)00228-5

Wang, Z. Q., Song, Q. Y., Su, J. C., Tang, W., Song, J. G., Huang, X. J., An, J., Li, Y. L., Ye, W. C., & Wang, Y. (2020). Caffeic acid oligomers from *Mesona chinensis* and their in vitro antiviral activities. *Fitoterapia* , *144*, 104603https://doi.org/10.1016/j.fitote.2020.104603

Wu, Y., Taylor, K. E., Biswas, N., & Bewtra, J. K. (1998). A model for the protective effect of additives on the activity of horseradish peroxidase in the removal of phenol. *Enzyme and Microbial Technology*, *22*(5), 315–322. https://doi.org/10.1016/S0141-0229(97)00197-X

Xu, P., Uyama, H., Whitten, J. E., Kobayashi, S., & Kaplan, D. L. (2005). Peroxidase-catalyzed in situ polymerization of surface orientated caffeic acid. *Journal of the American Chemical Society*, *127*(33), 11745–11753. https://doi.org/10.1021/ja051637r

Yan, Q., Tang, X., Zhang, B., Wang, C., Deng, S., Ma, X., Wang, C., Li, D., Huang, S., & Dong, P. (2019). Biocatalytic oxidation of flavone analogues mediated by general biocatalysts: Horseradish peroxidase and laccase. *RSC Advances*, *9*(23), 13325–13331. https://doi.org/10.1039/C9RA00470J

Yang, F., Yu, P. Y., Zhao, J., Zhao, Y., & Wang, J. P. (2015). Intermolecular hydrogen bonding structural dynamics in ethylene glycol by femtosecond nonlinear infrared spectroscopy. *Acta Physico-Chimica Sinica*, *31*, 1275–1282.

Yu, Q., Fan, L., & Duan, Z. (2019). Five individual polyphenols as tyrosinase inhibitors: Inhibitory activity, synergistic effect, action mechanism, and molecular docking. *Food Chemistry*, *297*, 124910https://doi.org/10.1016/j.foodchem.2019.05.184

Zhu, Z., Luo, W., & Sun, D.-W. (2020). Effects of liquid nitrogen quick freezing on polyphenol oxidase and peroxide activities, cell water states and epidermal microstructure of wolfberry. *LWT*, *120*, 108923. https://doi.org/10.1016/j.lwt.2019.108923

Zwane, R. E., Parker, A., Kudanga, T., Davids, L. M., & Burton, S. G. (2012). Novel, biocatalytically produced hydroxytyrosol dimer protects against ultraviolet-induced cell death in human immortalized keratinocytes. *Journal of Agriculatural and Food Chemistry*, *60*(46), 11509–11517. https://doi.org/10.1021/jf300883h